JOURNAL OF GEOPHYSICAL RESEARCH, VOL. 103, NO. D20, PAGES 26,007–26,024, OCTOBER 27, 1998

Evaluation of recent precipitation studies for Greenland Ice Sheet

David H. Bromwich,[1] Richard I. Cullather,[2] and Qiu-shi Chen

Polar Meteorology Group, Byrd Polar Research Center, Ohio State University, Columbus

Beáta M. Csathó

Remote Sensing Laboratory, Byrd Polar Research Center, Ohio State University, Columbus

Abstract. The retrieval of an accurate spatial and temporal record of contemporary Greenland precipitation is a uniquely challenging task because of the extreme variability in both atmospheric processes and the resulting precipitation distribution over relatively small spatial scales. A comparison of precipitation data sets composed of monthly mean values from recent studies shows a convergence on the general features of the long-term spatial patterns but substantial disagreement on the temporal variability both regionally and for all of Greenland. There is general agreement on a long-term Greenland average of about 35 cm yr^{-1} and on long-term values for regional scales, although differences for outlying data sets exceed 50% of the observed glaciological estimate for particular regions. A fundamental problem is the inadequate topographic representation of Greenland in the numerical analyses. Nearly all of the data sets are overly dry for high-elevation areas, as seen from comparisons with glaciological observations from Summit. The east-central region of Greenland is found to be particularly susceptible to the temporal discontinuities in data sets which employ operational analyses. In contrast, there is strong agreement among all methods on the temporal variability for the west-central region over a 15-year period. From the comparison it is concluded that none of the data sets is able to capture all of the regional-scale features. In general, however, the deficiencies of each data set are readily identifiable from comparison and evaluation in the context of circulation features. Agreement among the methods on particular regions and timescales gives increased confidence in drawing conclusions related to aspects of Greenland's precipitation climatology. In particular, an enhanced precipitation retrieval method is found to be less susceptible to data artifacts than other methods using operational analyses. In the north, anomalously high precipitation is associated with cyclonic development near the Fram Strait. For west-central Greenland the close agreement among methods is related to the dominant contribution of the mean circulation.

1. Introduction

Greenland precipitation is an important climate variable with significant relevance to a variety of research interests. For reference, Figure 1 shows the location of Greenland and significant geographic features. Approximately 80% of Greenland's total area is covered by glaciers which have a maximum thickness of almost 3 km. Analyzed ice cores from Summit (72°N, 38°W) indicate that abrupt climate changes have occurred during and near the end of the last ice age [e.g., *Alley et al.*, 1993]. Recent investigations have suggested that rapid, large-scale climate change results from a bimodal nature in the North Atlantic thermohaline circulation that is affected by surface salinity [*Broecker*, 1997]. The surface salinity is a by-product of the regional hydrologic cycle, including local precipitation and nearby glacier runoff and discharge. Before a complete knowledge of this system and its sensitivities is achieved however, it will be necessary to understand the present-day precipitation regime and its controls and to document the recent variability. An understanding of the physical mechanisms responsible for modern precipitation trends is also necessary if the recently observed variability is to be related to the long-term predictions of recent modeling studies [*Ohmura et al.*, 1996; *Thompson and Pollard*, 1997].

Observational methods have practical limitations for providing uniform spatial and temporal data. Gauge observations have been shown to be effective in qualitatively describing the average local annual cycle [*Calanca and Ohmura*, 1994; *Berthelsen et al.*, 1993], however they are limited to coastal regions. There are also serious problems associated with the gauge collection of solid precipitation which prevent a quantitative assessment [*Woo et al.*, 1983]. As a result, precipitation data sets which rely on gauge measurements, such as the Global Precipitation Climatology Centre (GPCC) climatology [*Rudolph et al.*, 1994] (Figure 2), have difficulty in capturing the large-scale features present in glaciological syntheses.

In contrast to gauge data, accumulation measurements based on glaciological methods are generally considered reliable

[1]Also at Atmospheric Sciences Program, Department of Geography, The Ohio State University, Columbus.

[2]Now at Department of Aerospace Engineering Sciences, University of Colorado, Boulder.

Paper number 98JD02278.
0148-0227/98/98JD-02278$09.00

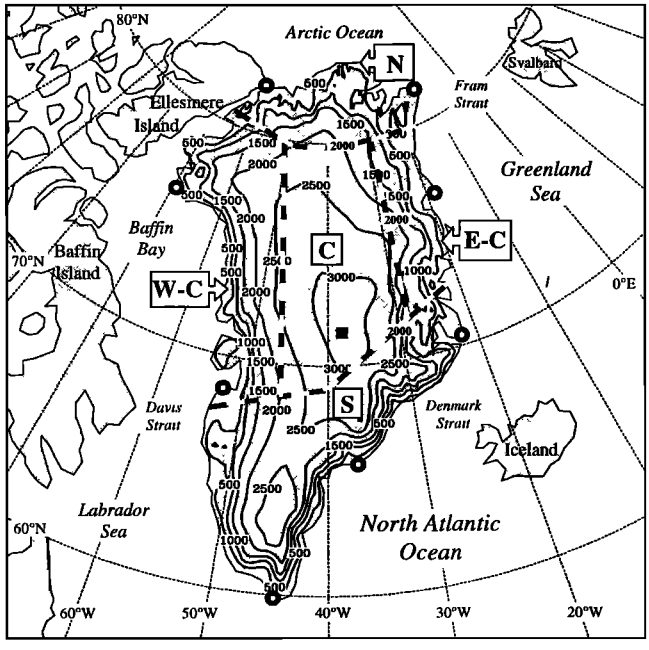

Figure 1. Geographic features surrounding Greenland. The topography for Greenland only is contoured using the Matrikelstyrelsen and Ekholm elevation map [*National Snow and Ice Data Center*, 1997] reduced to 0.5° x 0.5° resolution and contoured every 500 m. Circles indicate the location of Greenland rawinsonde stations [*Robasky and Bromwich*, 1994]. A solid square indicates the location of Summit. Dashed lines indicate boundaries for north (N) west-central (W-C), central (C), east-central (E-C), and south (S) regions examined.

[e.g., *Schwerdtfeger*, 1984]. At present, however, the glaciological observations represent a wide range of temporal sampling, and only long-term syntheses are available. Additionally, gauge measurements of solid precipitation are used for the nonglacial coastal margins to supplement the glaciological depiction [*Ohmura and Reeh*, 1991]. Figure 3 shows the Csathó-PARCA (Program for Arctic Regional Climate Assessment) accumulation map [*Csathó et al.*, 1997], a recent reexamination of the available data. The compilation is an objective analysis of the accumulation observations available to *Ohmura and Reeh* [1991] with the inclusion of a few recent measurements. Additional enhancements to this depiction are expected with the improved spatial coverage of glaciological observations supplied by the PARCA study.

These limitations have given rise to the use of several different atmospheric methods for examining precipitation variability over Greenland. Atmospherically derived precipitation estimates typically rely on atmospheric numerical analyses in order to retrieve values. The high spatial and temporal resolution furnished by these methods provides a valuable climatological record that cannot presently be obtained from other sources. Atmospheric data also provide an additional benchmark for satellite-based estimates of accumulation [e.g., *Zwally and Giovinetto*, 1995; *Shuman et al.*, 1995]. In this paper we examine the various atmospheric methods presently available for precipitation retrieval over this Arctic ice sheet in comparison to glaciological data and to each other. Similarities and discrepancies among the various methods are documented, and conclusions are drawn regarding the quality and usefulness of each method, as well as the implications of the noted discrepancies.

2. Methods

For the interior Greenland Ice Sheet, precipitation is related to accumulation using

$$\langle \overline{B} \rangle = \langle \overline{P} \rangle - \langle \overline{E} \rangle - \langle \overline{D} \rangle \tag{1}$$

where angled brackets represent an areal average, and the overbar represents a time average, B is accumulation, P is precipitation, E is the net of sublimation minus deposition of hoarfrost, and D is the divergence of snow drift. The equation is valid for the interior. At lower elevations the dominant impact on B is the net divergence of meltwater runoff. The drift snow term has been evaluated by *Loewe* [1970], who determined that D amounts to 1% or less of the mean annual accumulation for the whole of the Greenland Ice Sheet. The first two terms on the right-hand side are referred to as net precipitation (precipitation minus net sublimation). The dominant term in (1) is precipitation, and to a first order, the spatial distributions of B, P, and P–E have been thought to be comparable [e.g., *Chen et al.*, 1997].

2.1. Atmospheric Moisture Budget

Values of P–E for Greenland as a whole have been computed using the available rawinsonde network via the atmospheric moisture budget [*Robasky and Bromwich*, 1994]. The atmospheric moisture budget may be written as

$$P - E = -\frac{\partial W}{\partial t} - \nabla \cdot \int_{P_{top}}^{P_{sfc}} qV \, dp \tag{2}$$

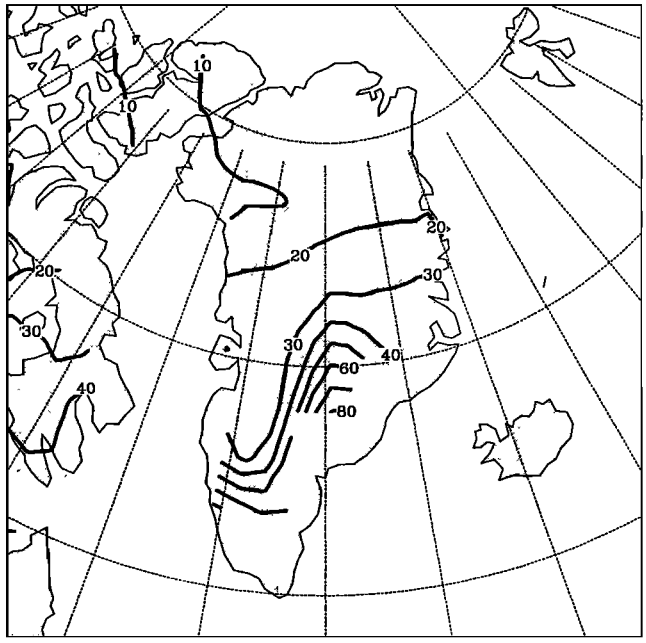

Figure 2. Average annual spatial distribution of the GPCC precipitation climatology [*Rudolph et al.*, 1994] for 1986-1995. The contour interval is 10 cm yr^{-1} water equivalent.

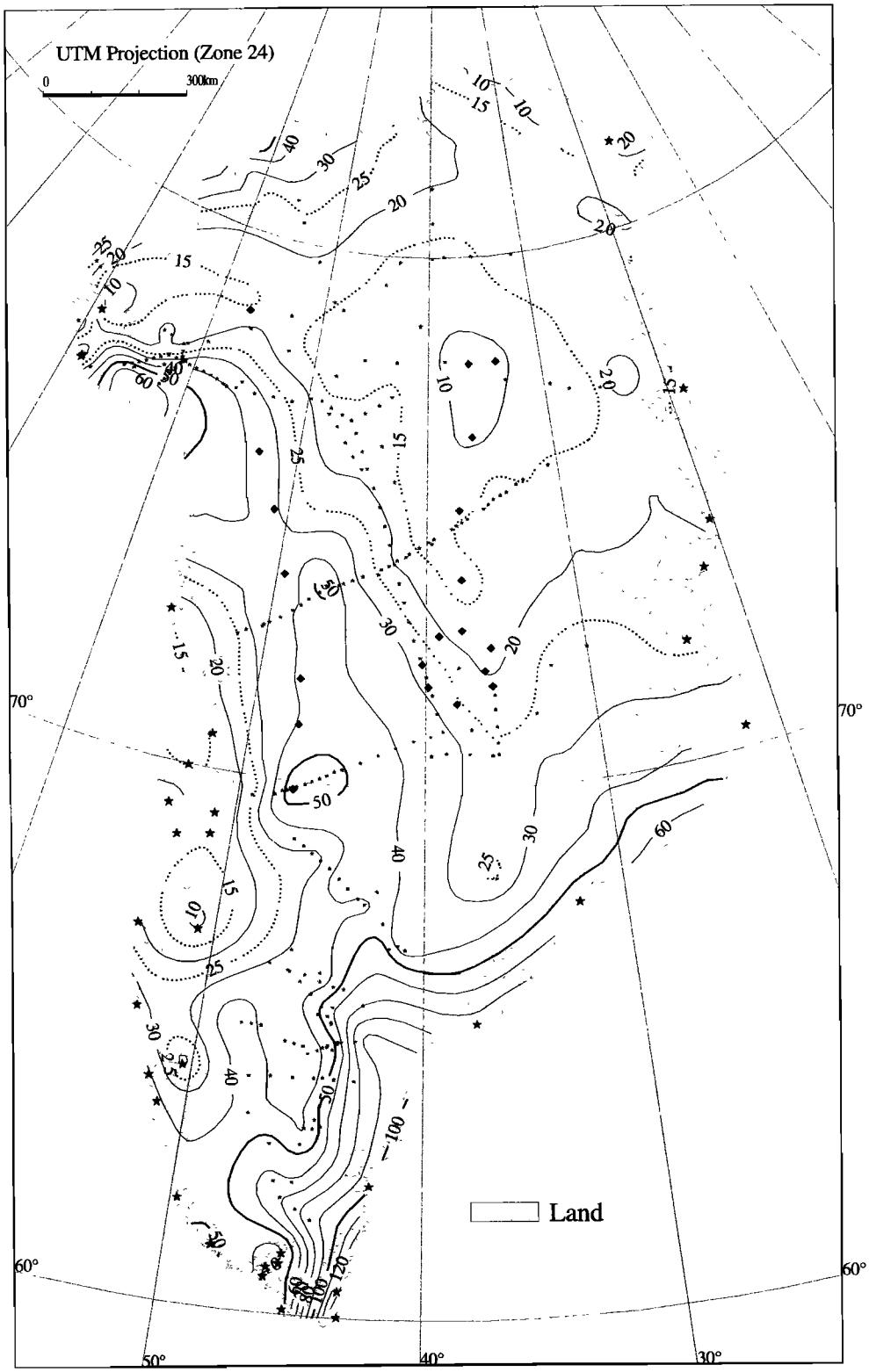

Figure 3. Csathó-PARCA accumulation distribution for Greenland [*Csathó et al.*, 1997]. Observational data points are indicated as small stars. Large stars indicate coastal gauge stations. Recently available data points are indicated as solid diamonds. The contour interval is 5 cm yr^{-1} water equivalent for values less than 30 cm yr^{-1} and 10 cm yr^{-1} for values greater than 30 cm yr^{-1}.

where W is precipitable water, P_{sfc} is surface pressure, q is specific humidity, and V is the horizontal wind vector. The variable P_{top} is the highest available measured pressure level of the atmosphere. An additional Reynolds decomposition of the second right-hand-side term into monthly mean and eddy components may be performed after temporal averaging of (2) using the covariance of q and V:

$$\overline{qV} = \overline{q}\,\overline{V} + \overline{q'V'}, \tag{3}$$

where the transient term is defined as

$$\overline{q'V'} = \frac{\sum_{i=1,n}\left(q_i - \overline{q}\right)\left(V_i - \overline{V}\right)}{n} \tag{4}$$

The computation shown in (2) has been performed by *Robasky and Bromwich* [1994] for the period 1973-1988 using the Greenland rawinsonde network (Figure 1). Prior to 1981 it was found that the rawinsonde time series was affected by missing observations that preferentially occurred during high moisture transport events. After that year, values reasonably approximate estimates of the average accumulation of the Greenland Ice Sheet, indicating that the Greenland rawinsonde network captures the large-scale atmospheric moisture transport events.

Equation (2) may also be applied to numerical analyses to produce a field of P–E. The moisture budget from analyses has previously been examined from a global perspective [*Oki et al.*, 1993; *Trenberth and Guillemot*, 1995; *Dodd and James*, 1996]. *Trenberth and Guillemot* [1995] evaluated the European Centre for Medium-Range Weather Forecasts (ECMWF) and the National Centers for Environmental Prediction (NCEP) operational analyses for the period 1985-1993. Substantial differences between the two analyses as well as artificial trends were found but particularly in the tropics, where the effects of limited diurnal resolution and the model cumulus parameterization can be significant. For Greenland the atmospheric moisture budget has been evaluated using ECMWF operational analyses by *Hurrell* [1995] and by *Calanca and Ohmura* [1994] for the period 1989-1991. In *Calanca and Ohmura* [1994] the data were smoothed using a 500 km isotopic filter to mitigate the spurious effects that are present in the 2.5° x 2.5° grid point data which result from the aliasing of small-scale features [*Trenberth*, 1992, p. 80]. This is a limiting factor on the spatial resolution for this method. *Hurrell* [1995] truncated results in spectral format to T31 horizontal resolution. In general, *Calanca and Ohmura* found the long-term spatial patterns to be captured. For this study, moisture budget computations using the ECMWF operational analyses have been extended to cover for the period 1985-1995 using similar computational methods to *Calanca and Ohmura* [1994].

2.2. Forecast Fields of the Reanalyses

Both the ECMWF and the NCEP have produced "reanalysis" data sets, in which the numerical weather prediction model and data assimilation system have been fixed over an extended period in time. This removes spurious trends in the data resulting from changes to the data scheme. Sources of temporal variability in reanalysis data are then limited to either real atmospheric variability or changes in the observational networks. The ECMWF reanalysis (ERA) [*Gibson et al.*, 1996] is a 15-year data assimilation product for the period 1979-1993. The ERA assimilation system employs an optimum interpolation of available meteorological observations, combined with a "first guess" field produced using a forecast model with T106 horizontal spectral resolution and 31 vertical hybrid levels. The NCEP/NCAR (National Center for Atmospheric Research) reanalysis [*Kalnay et al.*, 1996] is produced at T62 horizontal spectral resolution and 28 vertical sigma levels. The NCEP/NCAR reanalysis data set presently covers the period 1958-1996. In addition to numerical analyses, short-term analysis-initialized forecasts have been produced as part of operational and reanalysis data sets. This provides supplementary fields, including P and E, which are not directly observed or analyzed. These fields, however, are more dependent on the physics of the numerical weather prediction model utilized. The ERA supplementary fields are sampled during the 12- to 24-hr period of each forecast, while the NCEP/NCAR reanalysis are available for the 0- to 6-hour forecast. These data have been obtained from NCAR at 2.5° x 2.5° horizontal resolution.

The ECMWF operationally forecast P and E fields have been evaluated by *Genthon and Braun* [1995] for the period 1985-1991. On the basis of comparisons with glaciological data, *Genthon and Braun* [1995] conclude that the forecast fields do "a fairly good job" at reproducing the accumulation values. Forecast fields of the ECMWF reanalysis (ERA) and the NCEP/NCAR reanalysis have been previously evaluated on a global basis [*Stendel and Arpe*, 1997]. Greenland is not specifically discussed; however, comparisons of the average annual cycle with Russian north polar drift camp stations show reasonable agreement with the ERA and other gauge-based climatologies, while the NCEP/NCAR reanalysis overestimates values during June and July.

Over Greenland the NCEP/NCAR reanalysis precipitation field has been evaluated by *Chen et al.* [1997]. In high latitudes the field contains a spurious pattern resulting from the analysis model's parameterization of horizontal diffusion on constant pressure surfaces. This problem is manifested as a series of bull's-eyes oriented along meridians, which are amplified in the presence of steep topography. A particularly unfortunate result is the presence of a bull's-eye maximum located over the desertlike interior near Summit. The NCEP/NCAR precipitation field has also been examined by *Serreze and Maslanik* [1997] over the Arctic. A reasonable spatial distribution was obtained by filtering the data to a lower resolution. Recently, a corrected precipitation climatology has been produced by NCEP, which is also considered below. A corrected evaporation/sublimation field is not available, however. The forecast evaporation/sublimation field contains a similar pattern as the result of this deficiency's realization in the model cloudiness field and in other moisture variables; in light of these problems we defer consideration of forecast evaporation/sublimation fields.

A first-order evaluation of the evaporation/sublimation component may be obtained by examining the ERA forecast E field, shown in Figure 4. For the annual average, E is very small and appears to be of some significance only for the southern region and the far north where values begin to approach the same order of magnitude as P. For the interior regions, annually averaged E is slightly negative (deposition). The values of E shown for the margins are significantly smaller than have been reported in a GCM study [*Thompson and Pollard*, 1997], although near-surface air temperatures for

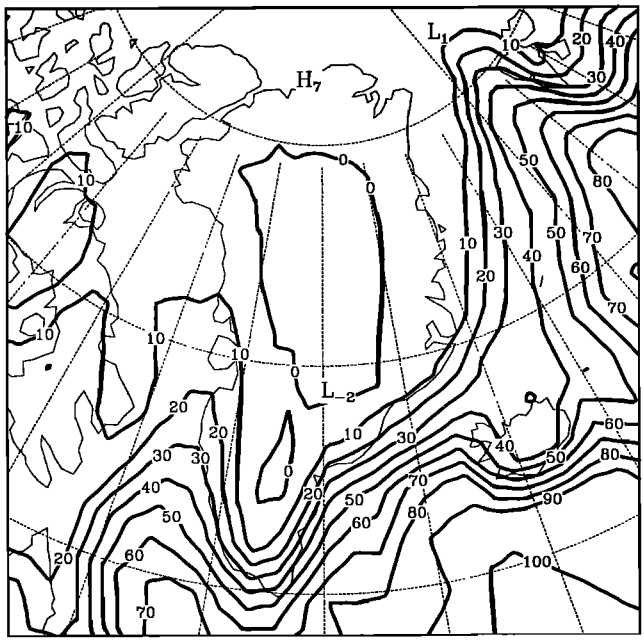

Figure 4. Average annual spatial distribution of forecast E from the ERA data set for 1979-1993. The contour interval is 10 cm yr^{-1}.

their simulation were found to be too warm. During the Greenland Ice Margin Experiment (GIMEX) [*van den Broeke et al.*, 1994; *Meesters*, 1994] the surface energy balance was observed in southwestern Greenland during the summer of 1991. The primary motivation was the radiation balance however, and published latent heat flux values either apply to individual days (e.g., July 12, 1991) or contain large uncertainties [*Duynkerke et al.*, 1994]. Values from previous observational studies by W. Ambach have been referenced for camps near 70°N, 48°W for June and July 1959 and 1967 [*Duynkerke and van den Broeke*, 1994], and these have been compared with the ERA data. The computed rates of E from the two observation years are 17±4 cm yr^{-1} for June and 13±2 cm yr^{-1} for July. For the period 1979-1993 the corresponding ERA values for this location are 14±1 cm yr^{-1} and 25±1 cm yr^{-1} for June and July, respectively. Additionally, these values occur in the presence of a large spatial gradient; given this and the potentially large interannual variability, the ERA values seem to be reasonable. In general, the depiction of E shown in Figure 4 appears to be realistic in comparison to the limited amount of validation data currently available.

2.3. Enhanced Precipitation Retrieval

A new source of Greenland precipitation data using numerical analyses, which has been recently explored, is known as "enhanced precipitation retrieval." This makes use of a digitized Greenland topography to retrieve precipitation at a higher spatial resolution than is available through other methods. Two applications of this approach are examined here. The first application is an initial study of the topic conducted by *Bromwich et al.* [1993]. The method used, referred to as the Keen model [*Keen*, 1984], employed a parameterization of 500 hPa synoptic activity with a simple orographic scheme given as

$$P = A_0 q_{700} |\mathrm{VFI}| + A_1 q_{700} V_{850} \cdot \nabla H \quad (5)$$

where A_0 and A_1 are empirical coefficients, q_{700} is the 700 hPa specific humidity, V_{850} is the computed 850 hPa horizontal geostrophic wind, and H is the surface topography. The vorticity flux index (VFI) is determined from the filtering of the 500 hPa geopotential height field. The first term on the right-hand side, an expression of positive vorticity advection, is referred to as the dynamic component and provides the vertical velocity in an equivalent-barotropic atmosphere. The coefficient for the dynamic precipitation component A_0 was determined using an accumulation time series for Summit [*Bolzan and Strobel*, 1994]. Thus the model is "tuned" for this location. The second term is referred to as the orographic component; the orographic component coefficient A_1 was also determined using accumulation data. Using operational analyses of the National Meteorological Center (NMC, now NCEP), precipitation was computed for the period 1964-1988. In comparison to long-term glaciological estimates, the Keen model was found to reproduce major spatial characteristics of the observed accumulation.

A second application of enhanced precipitation retrieval is the Chen-Bromwich precipitation data set [*Chen et al.*, 1997]. The Chen-Bromwich method utilizes ECMWF operational analyses to produce a precipitation depiction with 50 km resolution. The method is illustrated in Figure 5. The principal inputs to the model are the ECMWF analyses and the

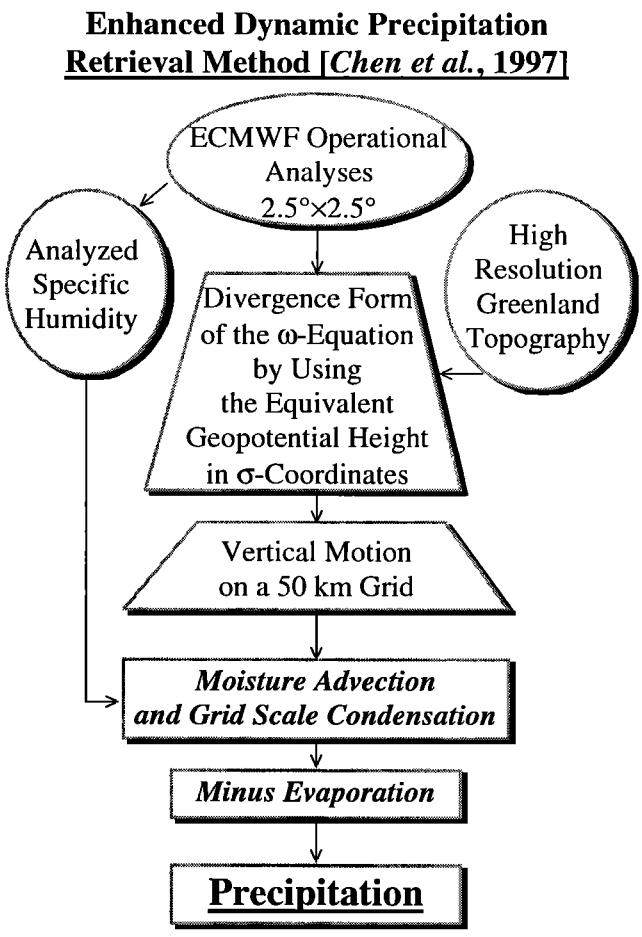

Figure 5. Schematic diagram of the Chen-Bromwich enhanced precipitation retrieval model [*Chen et al.*, 1997].

Greenland topography. Using a generalized form of the ω equation in σ coordinates, a vertical motion field at high spatial resolution is obtained. From the three-dimensional wind field and analyzed variables the large-scale condensation and evaporation for atmospheric layers are then computed, resulting in precipitated rain or snow if the lowest atmospheric level is saturated.

3. Spatial Distribution

The spatial distribution of the long-term accumulation field synthesized from glaciological data has previously been described by *Ohmura and Reeh* [1991] and *Csathó et al.* [1997]. The distribution shown in Figure 3 generally indicates larger values along the southeast coastline with a significant elevation-related gradient to very small values in the interior. A region of some interest is along the western glacier margins near the 2400 m elevation contour. Previous syntheses have shown an orographically-related precipitation maximum extending from near Jacobshavn (approximately 70°N, 47°W) northwest to near Thule (77°N, 69°W). A major source of information for this feature has been measurements from the 1912 to 1913 Swiss Greenland Expedition [*Ohmura and Reeh*, 1991]; however, the region has been heretofore undersampled. The recent addition of cores from PARCA to the accumulation distribution has diminished this feature (Figure 3), although there remains a significant east-to-west gradient across the center of the ice sheet. Only relatively larger values in close proximity to the location of the original measurements remain, rather than the continuous large-scale feature found in previous distributions. Nevertheless, values along the western half of Greenland north of 70°N are significantly larger than along the east coast.

Figure 6 shows the multiyear spatial distributions of each of the atmospheric methods. Essentially, all of the methods show two large-scale precipitation features for Greenland: desertlike conditions for the northern ice sheet dome and very large values of 100 to 200 cm yr^{-1} along the southeast coastal regions. The average spatial distribution of P–E derived from the atmospheric moisture budget using ECMWF operational analyses (Figure 6a) is very similar to the Csathó-PARCA depiction. Along the southeast coast, ECMWF moisture budget values are as large as 102 cm yr^{-1}. This appears to be slightly low in comparison to the accumulation synthesis. However, there are difficulties with the accumulation data along the extreme coastal margins because of limited observations and complex topography. North of 70°N the spatial distribution is again very reasonable in a broad sense. At the highest elevations, however, the region covered by the 10 cm yr^{-1} contour is substantially larger than is supported by glaciological studies (Figure 3); average values for the interior are too low. The remaining five panels show precipitation, which has been estimated to be 8% greater than the depicted accumulation for the whole of Greenland [*Ohmura and Reeh*, 1991; *Bromwich et al.*, 1993]. The ERA forecast precipitation shows values ranging from 182 cm yr^{-1} along the southeast coast to about 4 cm yr^{-1} in the interior. While the maximum values are not unreasonable in both location and magnitude, the minimum for the interior plateau is again too small. For example, the long-term average accumulation for Summit, which has been extensively sampled, is 22 cm yr^{-1} [*Bolzan and Strobel*, 1994], while ERA values averaged over 15 years are less than 50% of this value. A similar shortfall in ERA precipitation over polar glaciers has also previously been found for Antarctica [*Stendel and Arpe*, 1997]. Not surprisingly, there is a greater amount of detail in the averaged forecast precipitation than in the lower-resolution moisture budget data. This is particularly true along the western coast.

Figure 6d shows the average distribution of the corrected NCEP/NCAR reanalysis forecast precipitation. The original spatial distribution which has been discussed previously [*Chen et al.*, 1997] is shown in Figure 6c. A larger contour interval of 25 cm yr^{-1} is used for Figures 6c and 6d only to accommodate the large values. Erroneous higher-latitude maxima in the original NCEP/NCAR reanalysis precipitation data, which buttress Greenland near Thule and on the northeastern and northern coastlines, have been removed in Figure 6d. The correction identifies the bull's-eyes as spurious moisture sources and removes them in comparison to a diffusion-corrected moisture amount, subject to a temperature threshold. It is apparent from examination of the corrected field, however, that the problem is with the distribution, rather than the amount of atmospheric moisture. The corrected precipitation field, although an improvement in the spatial distribution, is overly dry in comparison to the original field and the ERA north of 70°N. This leads to a contrast between northern and southern Greenland that is greater than for other methods. Additionally, over central Greenland the temperature threshold of the correction does not allow for the complete removal of the spurious maximum that extends over the relatively colder regions of the high plateau. In general, neither of the two spatial depictions available from the NCEP/NCAR reanalysis appear to be promising.

Figure 6e shows the spatial pattern of the Keen model [*Bromwich et al.*, 1993]. The model uses NCEP operational analyses available on a polar stereographic grid that is diagonal to the view shown. The offshore values which increase to the south are in areas with minimal topographic forcing and are erroneous. Over the interior plateau the values shown are quantitatively superior to other methods. This is partially misleading, however, because the model was fitted to agree with glaciological data at Summit (i.e., coefficient A_0 of equation 5 [*Bromwich et al.*, 1993]). Significant differences exist with other climatologies along the southern coastal regions. A maximum value in the Keen data of 137 cm yr^{-1} is found near the Denmark Strait. Along the west coast a continuous string of maxima occurring in close proximity to the coastline is not supported by the glaciological depiction. Finally, Figure 6f shows the average spatial pattern of the Chen-Bromwich precipitation data. Both the Keen model and the Chen-Bromwich precipitation data have a significantly higher spatial resolution however; this is particularly apparent in the Chen-Bromwich distribution. Figure 6f is significantly busier than the other distributions. A resulting difference is the strong spatial gradient along the southeast coast, where the contour lines have merged together. Several maxima of up to 160 cm yr^{-1} are apparent along the southeast coastline. This falls to less than 30 cm yr^{-1} only a short distance inland. Over the interior the spatial distribution is very similar to that of the ERA, which features two areas of less than 10 cm yr^{-1}. Again, the values for the interior are small in comparison to the glaciological data. To an extent, the Chen-Bromwich precipitation data give the appearance of being a higher-resolution version of the ERA precipitation data. A feature well captured by the Chen-Bromwich model is the precipitation maximum near Thule.

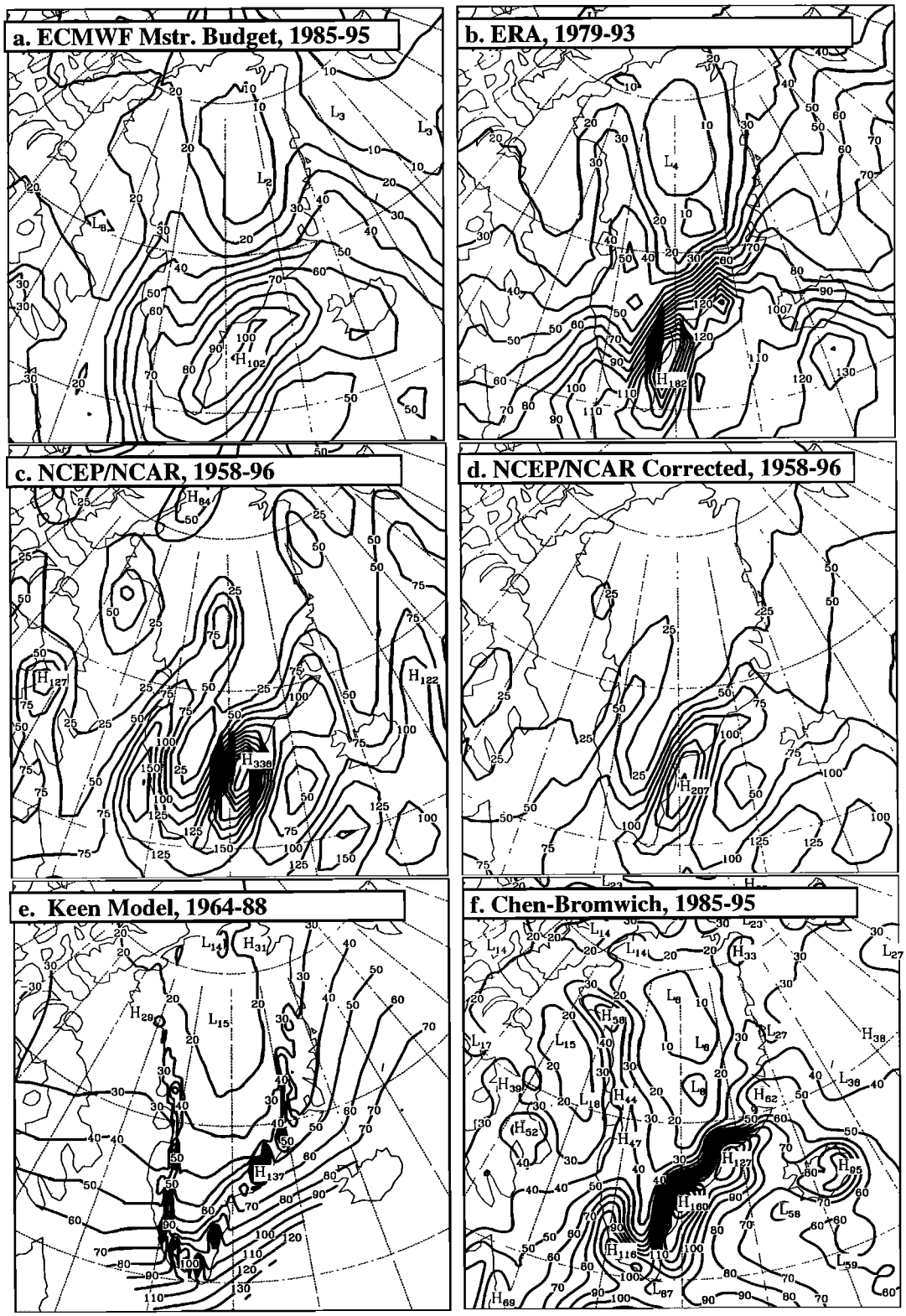

Figure 6. Average spatial distributions for various methods: (a) $P-E$ derived from the atmospheric moisture budget using ECMWF operational analyses for 1985-1995; (b) forecast precipitation from the ERA for 1979-1993; (c) forecast precipitation from the NCEP/NCAR reanalysis for 1958-1996; (d) a corrected forecast precipitation climatology from the NCEP/NCAR reanalysis for 1958-1996; (e) precipitation using the Keen model, 1964-88; and (f) precipitation from the Chen-Bromwich model for 1985-1995. The contour interval is 10 cm yr^{-1} for Figures 6a, 6b, 6e, and 6f, and 25 cm yr^{-1} for Figures 6c and 6d.

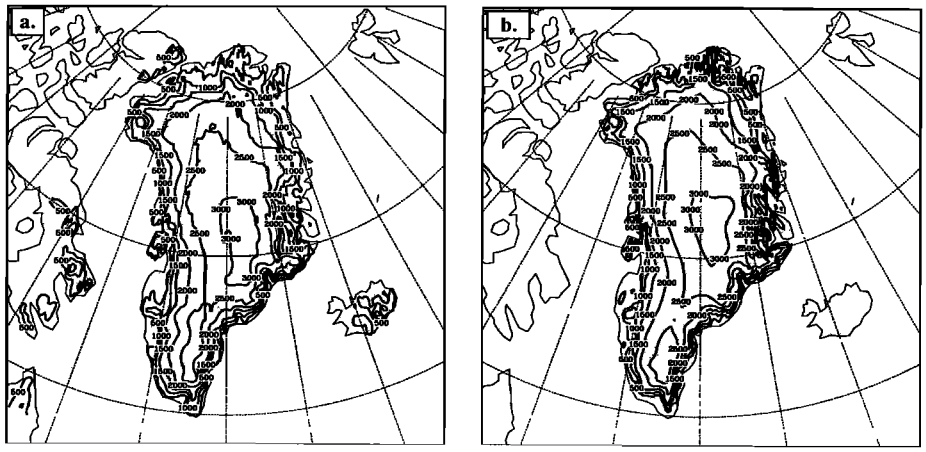

Figure 7. Comparison of topographies of (a) U.S. Navy elevation data set and (b) Matrikelstyrelsen and Ekholm elevation data [*National Snow and Ice Data Center*, 1997]. The contour interval is 500 m.

Several of the deficiencies in the spatial distributions are probably related to the topographic data employed in assimilation and modeling. Both the ECMWF and the NCEP use spectral versions of a global U.S. Navy 10 arc min digital elevation data set. *Chen et al.* [1997] also elected to use this data set for their study, while *Bromwich et al.* [1993] used a 20 km ice sheet terrain data set produced by *Radok et al.* [1982]. *Genthon and Braun* [1995] have identified substantial errors of up to 1 km in the U.S. Navy data set over the Antarctic ice sheet. A comparison of Navy topographic data with the Matrikelstyrelsen and Ekholm digital elevation field for Greenland, shown in Figure 7, also reveals significant discrepancies. The Matrikelstyrelsen and Ekholm field is a realistic digital elevation data set synthesized from a variety of observations including satellite radar altimetry [*Ekholm*, 1996]. The Navy depiction of the plateau region is found to erroneously extend too far to the south. Such an error would have the effect of increasing orographic precipitation closer to the southeast coastline while reducing the total amount of moisture transported inland. This generally describes the

Table 1. Comparison of Annual Precipitation Estimates for Greenland, in Centimeters Water Equivalent per Year

Quantity	Method	Data	Frequency	Time Span	Value, cm yr^{-1}
Accumulation	glaciological synthesis	*Bender* [1984]	--	long term	39.0
Accumulation	glaciological synthesis	*Ohmura and Reeh* [1991]	--	long term	31.0
Accumulation	glaciological synthesis	*Reeh* [1994], *Warrick et al.* [1995]	--	long term	32.0
Accumulation	glaciological synthesis	*Csathó et al.* [1997]	--	long term	30.2
P–E	atmospheric moisture budget	rawinsonde [*Robasky and Bromwich*, 1994]	twice daily	1980-1989	32.1±2.3
P–E	atmospheric moisture budget	ECMWF operational analyses [after *Calanca and Ohmura*, 1994]	twice daily	1985-1995	30.5±0.8
P	series of forecasts	ERA	averaged over each 12-24 hour forecast	1979-1993	33.5±0.7
P	series of forecasts	NCEP/NCAR reanalysis	averaged over each 0-6 hour forecast	1958-1996	39.1±0.7
P	series of forecasts	corrected NCEP/NCAR reanalyses	averaged over each 0-6 hour forecast	1958-1996	27.6±0.7
P	Keen model [*Bromwich et al.*, 1993]	NCEP operational analyses	daily	1964-1988	38.4±1.0
P	Chen-Bromwich model [*Chen et al.*, 1997]	ECMWF operational analyses	twice daily	1985-1995	37.6±1.2

Uncertainty in atmospheric methods is shown as the standard error for annual values in each time series.

characteristic deficiency of the methods shown in Figure 6. Closer inspection of the Navy data set has also revealed some unusual and, apparently, unwarranted detail in the vicinity of Summit. This appears to be partly responsible for the pattern of two minimum regions found in the ERA and Chen-Bromwich fields. Finally, significant discrepancies are found north of 80°N, where the Navy data set is up to 300 m too low.

Table 1 compares the various methods averaged for Greenland. The Greenland area is defined using the land-ocean masks of the various data sets. It should again be emphasized that the glaciological estimates shown represent the synthesis of various data corresponding to a variety of time periods; a glaciological synthesis for the whole island that is contemporaneous with atmospheric data is not presently available. Overall, there is a general agreement among the methods of approximately 35 cm yr^{-1}. However, it is not possible to draw conclusions regarding the magnitude of E and blowing snow divergence terms from the given sources of data, because the relative errors in the estimates of P and $P-E$ are likely to be larger than the difference of the two. Forecast precipitation from reanalysis data, for example, contains the effects of moisture spin-up within the model, so the forecast $P-E$ is generally not in agreement with the derived moisture budget from analyses [*Mo and Higgins*, 1996; *Trenberth and Guillemot*, 1996]. Moisture spin-up occurs as the model responds to imbalances in the initial fields [e.g., *Trenberth*, 1997]. The underestimation over the interior plateau by atmospheric methods is not sufficient to dominate the overall Greenland average. The mean value from atmospheric methods (34.1 cm yr^{-1}) is approximately 10% larger than that of recent accumulation studies. This is at least in the correct sense for compensation of the lesser terms of equation (1). All of the atmospheric methods are constrained to varying degrees by the accuracy of rawinsonde measurements of atmospheric moisture. This comparison supports the conclusion that well-known difficulties in measuring humidity at low air temperatures [e.g., *Elliott and Gaffen*, 1991] are mitigated in the computation of moisture convergence [*Robasky and Bromwich*, 1994].

4. Temporal Variability

The major weather system producing precipitation over Greenland is the frontal cyclone [*Chen et al.*, 1997]. As a result of the transient nature of cyclonic activity, an irregular annual cycle develops for the whole of Greenland. Figure 8 shows the average annual cycle of four methods examined during the overlapping years 1985-1993. On average, March has the minimum amount of precipitation, and a maximum is found during autumn months. There is a great deal of variability from year to year; however, in general, the minimum precipitation month occurs between December and April. This must be put into context of the annual cycling of the significant storm tracks, however. Because of the varying cycles and the centers of action, there is a significant spatial variability to the annual cycle. For example, the southern region is strongly influenced by the North Atlantic storm track which becomes active during winter months, producing a maximum in southern coastal gauge data in December [*Berthelsen et al.*, 1993]. In contrast, the Arctic coastal regions experience an annual precipitation cycle that is essentially in opposite phase to the south. To better understand the various Greenland precipitation regimes and the performance of the various methods, time series have been developed from the various data for five regions shown in Figure 1. These regions are defined by *Chen et al.* [1997], based on the subjective examination of synoptic precipitation over 2 years. Glaciological study also supports a similar partitioning [*Fisher et al.*, 1996]. It is clear from the deficiencies shown in Figure 6 that the NCEP/NCAR forecast P will encounter significant difficulties at higher spatial resolution, and therefore only the corrected NCEP P fields are

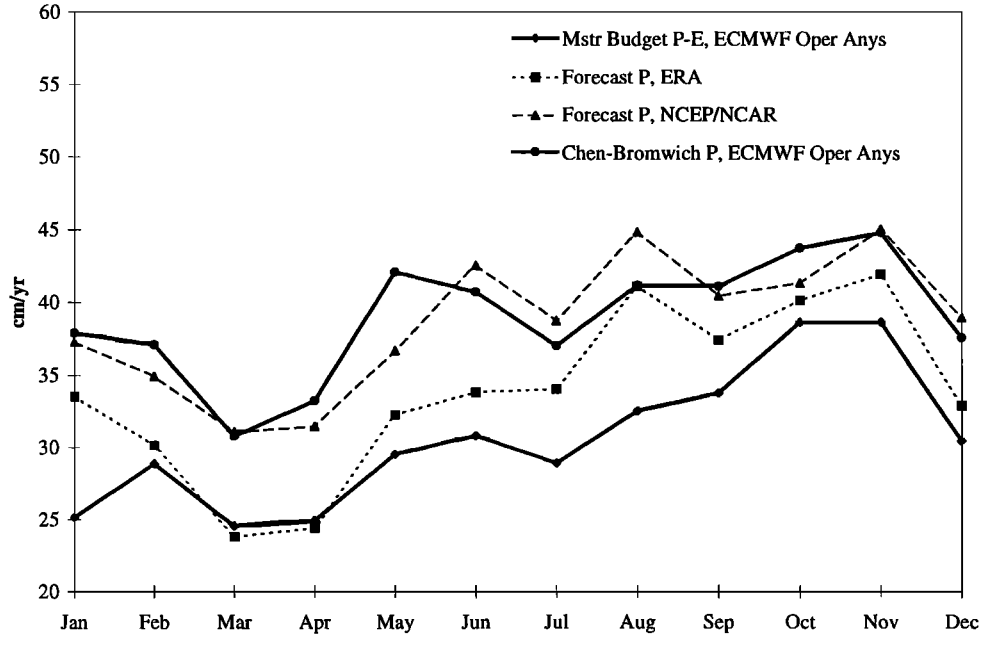

Figure 8. Monthly mean precipitation values for Greenland from four data sets, averaged for 1985-1993, expressed as the rate of cm yr^{-1}.

Table 2. Comparison of Regional Precipitation Estimates, in Centimeters per Year Water Equivalent for Years 1985-1993

	North	West-Central	Central	East-Central	South
Accumulation, Csathó-PARCA synthesis	19.9	29.2	21.1	18.2	44.0
P–E, ECMWF oper. anys. moisture budget	10.2	31.0	15.6	13.7	59.0
P, ERA forecasts	11.1	33.2	13.6	17.7	69.0
P, corrected NCEP/NCAR forecasts	7.7	24.5	11.7	13.3	57.8
P, Keen model (available through 1988)	21.1	25.6	18.0	29.0	57.9
P, Chen-Bromwich	23.6	32.5	10.4	27.1	76.0

examined regionally. Below, each of the five areas are considered in more detail, and Table 2 summarizes this comparison.

4.1. Northern Greenland

The Arctic coastline region lies north of the 80° parallel with monthly averaged surface temperatures experiencing an average range of between −35°C for December to March and −3°C in July, as computed from ECMWF analyses. Because of the topography, many cyclonic systems occurring to the south are effectively blocked by the ice sheet dome from affecting the northern region. Annual precipitation values are extremely small. Cyclonic patterns for this region have been reviewed by *Bradley and Eischeid* [1985] and *Chen et al.* [1997]. See *Serreze and Barry* [1988] for a basin-wide review of Arctic cyclonic activity. There is no high-frequency storm track which affects northern Greenland. In summer, however, transient cyclones have previously been found to move from the Beaufort Sea across the Canadian archipelago, or move northeast after development in the Baffin Bay region. *Bradley and Eischeid* [1985] also indicate that the most predominant synoptic condition for enhanced precipitation in the Canadian high Arctic is the presence of slow-moving high pressure centered south or southwest of Ellesmere Island, resulting in deposition through moisture advection and orographic lifting. These synoptic conditions are highly episodic in nature but preferentially produce larger precipitation amounts during summer months. Larger summertime precipitation may also be related to the presence of reduced sea ice concentration in the Canada basin, which is described by *Serreze et al.* [1989].

A comparison of the various climatologies generally shows considerable disagreement in annual values averaged over the period 1985-1993. In general, the enhanced precipitation retrieval methods show values which are more than twice that of either forecast reanalysis products or the atmospheric moisture budget method. As shown in Table 2, the ERA forecast *P* averages 11 cm yr^{-1}, while the Chen-Bromwich precipitation model averages 24 cm yr^{-1}. These higher values for the northern region produced by the enhanced precipitation retrieval methods are supported by the long-term glaciological synthesis, which averages about 20 cm yr^{-1}. Again, the corrected NCEP forecast *P* values are considerably smaller than all other methods for the northern region, averaging 7.7 cm yr^{-1}. For all methods the standard error of annual values is less than 1.4 cm yr^{-1}. There is first-order agreement on an annual cycle however, which is composed of larger values in summer. To more closely examine differences in the annual cycle, a seasonality index is developed as the ratio of precipitation for June, July, and August divided by the December, January, and February precipitation. The index again shows differences between enhanced precipitation retrieval methods and the other methods. Seasonality is slightly less for the enhanced methods, with an average index value of 2.2 for the Chen-Bromwich precipitation retrieval method and 3.0 for ERA forecast *P*. The data from the ECMWF atmospheric moisture budget method have a seasonality index of 2.9. This index value for *P–E* is very close to the previous estimates for *P*, and thus it is unclear as to whether the seasonal variability in *E* is significant. The corrected NCEP precipitation field has a seasonality index of 5.1, which perhaps results from the temperature dependency criterion used in the correction scheme.

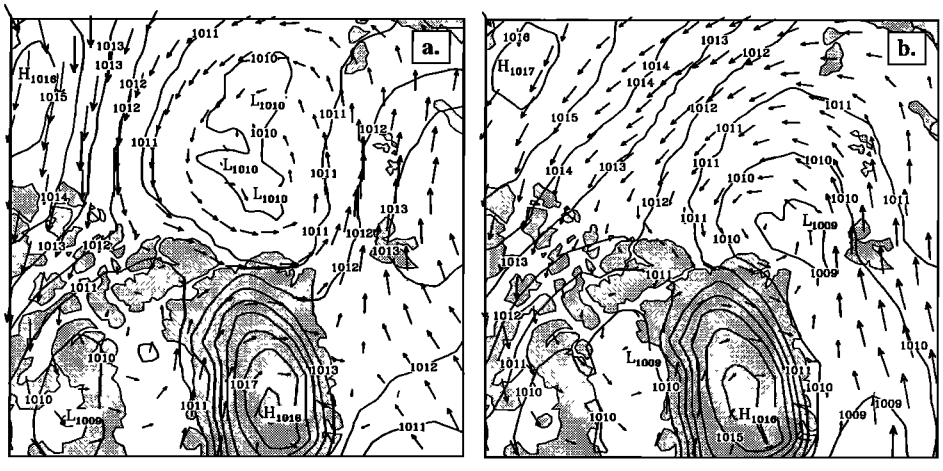

Figure 9. Comparison of sea level pressure and vertically integrated moisture transport vectors from ECMWF operational analyses averaged for (a) average conditions for summer (JJA) months and (b) northern Greenland enhanced precipitation months. The enhanced precipitation months are June 1988, July 1987, July 1991, April 1990, September 1991, June 1992, September 1990, August 1991, July 1985, and June 1987. Sea level pressure is contoured every 1 hPa.

There is some disagreement between the various methods for the year-to-year variability in the northern region. For example, the ECMWF moisture budget shows a substantial upward trend of about 1.1 cm yr^{-1} for the years 1985-1993, while the other methods show little or no trend. Three data sets, the ERA, corrected NCEP, and the Chen-Bromwich data, all show similar variability in annual values, with significant correlations between the Chen-Bromwich and corrected NCEP annual values (r^2=0.35) and the ERA and corrected NCEP values (r^2=0.65). Discrepancies are due to the winter months, when the values are so low as to become significantly affected by artificial factors such as changes to the data assimilation scheme.

Each time series generally reflects the episodic nature of the precipitation events, with about a dozen months having significantly larger values than the rest of the time series. These higher precipitation months generally occurred in summer. For the time period 1985-1993, the 10 highest precipitation months from the moisture budget, reanalysis data, and Chen-Bromwich data set were selected from each time series. There was considerable agreement among the methods as to which 10 months were the largest as well as the order, and an overall composite list of 10 months was produced. Figure 9 indicates the circulation conditions present during these months in comparison to average summer conditions. The typical summer pressure distribution indicates a minimum centered very close to the pole. This climatological low is essentially barotropic, and the averaged atmospheric moisture transport follows a zonal pattern around the Arctic Basin. In this configuration the amount of moisture transported to Greenland from the direction of the Canadian archipelago is minimal. During enhanced precipitation months, the low occupies a location northeast of Greenland near Svalbard, and the moisture flux appears to respond to an onshore flow and arrives on the ice sheet from a more northerly source. This confirms the analysis of *Chen et al.* [1997] who examined the circulation characteristics over a 2-year period. The synoptic characteristics producing these events cannot easily be determined from the mean fields. Again there is no high-frequency storm track which directly affects northern Greenland; however, the patterns which produce precipitation can be resolved by comparing the synoptic variability for high precipitation months with average summer conditions. First, a bandpass filter is used to filter sea level pressure data for synoptic timescales [*Duchon, 1979*]. Computing the root-mean-square of the filtered data then produces a spatial depiction of the synoptic variability for each month. In Figure 10, average synoptic variability depictions for summer months are subtracted from the depictions for high precipitation months. The difference plot indicates increased synoptic activity along the northeast coast in addition to systems moving in from the west. An examination of the individual analyses for a few of the months indicates systems moving north along the eastern coast of Greenland or cyclogenesis occurring along the northeastern coast. There is some evidence to indicate that some systems developing in Baffin Bay are actually able to cross over the ice sheet and redevelop in the Fram Strait, a behavior that has been previously noted for winter months [*Keegan*, 1958]. Two extreme cases were also found for June 1988 where cyclones passing through the Fram Strait began a retrograde motion, traveling west along the northern coast of Greenland.

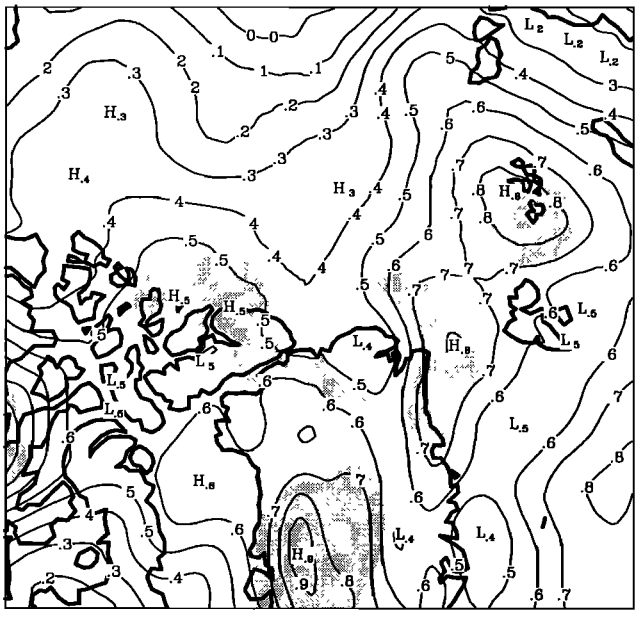

Figure 10. Monthly RMS of the synoptically filtered sea level pressure field, averaged for 10 months of enhanced northern Greenland precipitation, minus corresponding values averaged for all summer months (JJA) for 1985-1993. The contour interval is 0.1 hPa. Shaded areas correspond to the 95% confidence interval determined by Student's *t*-statistic.

4.2. West-Central Greenland

Chen et al. [1997] have previously reviewed synoptic conditions leading to precipitation along the western coast of Greenland. The west-central region is susceptible to synoptic activity moving northeast out of central Canada, developing in Baffin Bay, or progressing north into Baffin Bay from the North Atlantic.

For the precipitation climatologies the west-central region is notable for its agreement among all methods for a variety of timescales. For the years 1985-1993 the average value for all methods is approximately 29 cm yr^{-1}, which is in agreement with the long-term glaciological synthesis, as shown in Table 2. Two methods that significantly differ from this value are the Keen model, with an average value for 1985-1988 of 26 cm yr^{-1}, and the NCEP precipitation average of 25 cm yr^{-1}. The lower value for the Keen model is consistent with previously examined deficiencies in the spatial pattern along the west coast in comparison to glaciological data noted by *Bromwich et al.* [1993]. *Serreze and Barry* [1988] concluded that the NCEP octagonal analyses used by the Keen model were of insufficient horizontal resolution to capture Baffin Bay systems. Figure 11 shows the averaged annual cycle. The annual cycle is highly variable; however, there is considerable agreement on a mean cycle composed of higher values in late summer or early autumn and lower values in late winter or early spring. This is qualitatively in agreement with gauge measurements from coastal stations [*Berthelsen et al.*, 1993].

Interannual variability also shows close agreement among the various methods. Figure 12 shows several time series of the annual values for 1980-1995. All methods agree on a downward trend after the largest values were obtained in 1986. From Figure 12 the agreement between the time series in

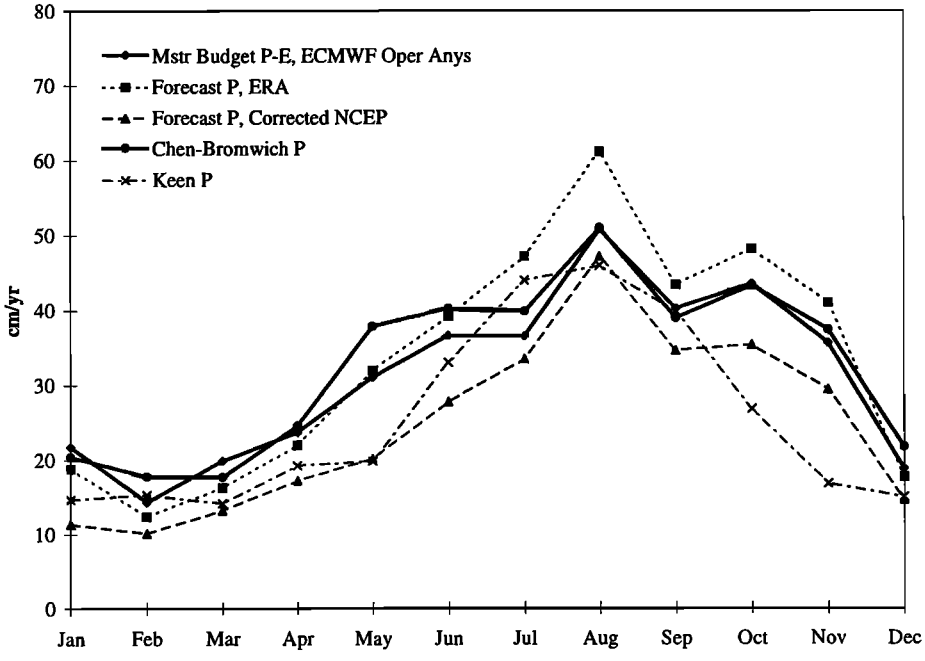

Figure 11. Average annual cycle of various precipitation methods for the region defined as west-central in Figure 1 for 1985-1993, in cm yr^{-1}.

Figure 12 has been assessed by computing r^2 for each pairing of the methods. The average r^2 for all of these pairings is 0.52; excluding pairings with the Keen model, the average comparison is very close (average r^2=0.72) with little variation.

The exceptional agreement among the various methods suggests precipitation for west-central Greenland is subject to controls which are reproducible by all of the methods. *Calanca and Ohmura* [1994, Figure 3] have shown this region to be dominated by the mean component of the atmospheric moisture transport, with a regional minimum in transient moisture flux convergence. The deficiencies of the NCEP octagonal grid data in representing Baffin Bay cyclone activity limit the performance of the Keen model; however, most of the precipitation in this region is due to mean transport and orographic lifting, which appear to be adequately resolved by all of the methods. The comparison of mean versus eddy moisture convergence is discussed in more detail for the east-central region. This agreement between methods strengthens confidence in previous findings of a precipitation

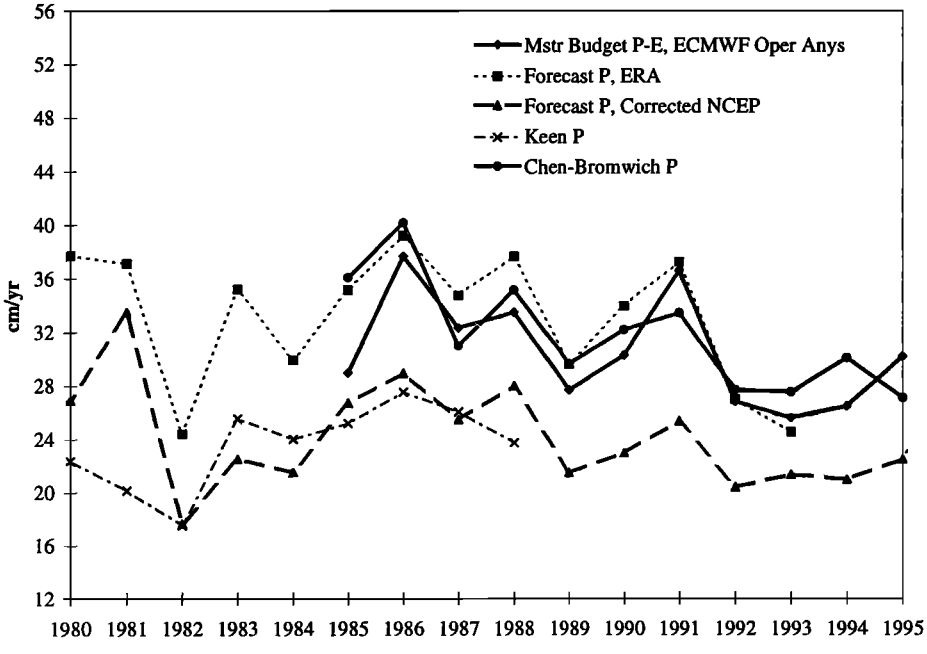

Figure 12. Time series of annual values for various precipitation methods for the region defined as west-central in Figure 1, in cm yr^{-1}.

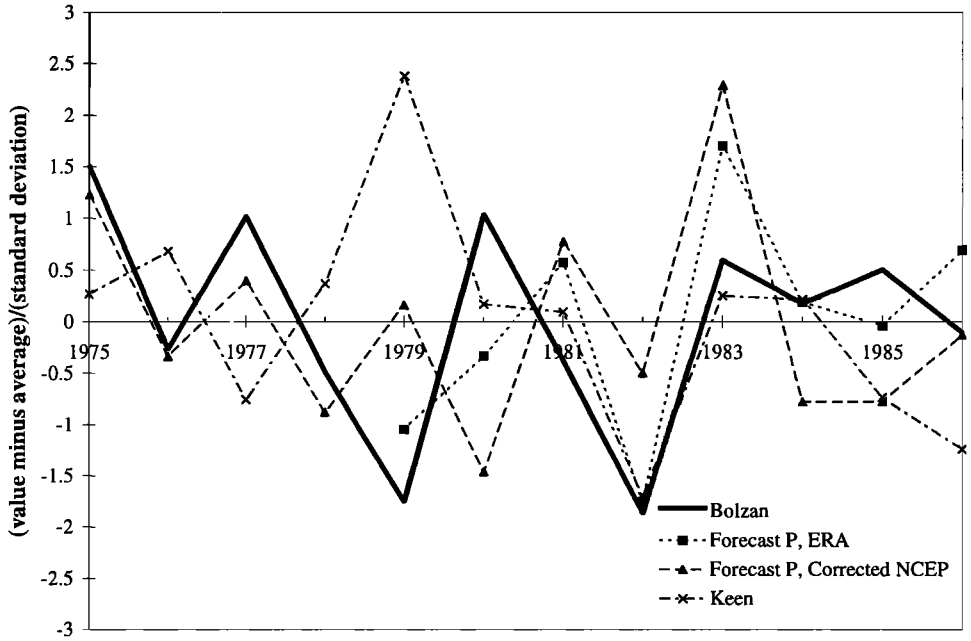

Figure 13. Time series of normalized annual values for various precipitation methods and accumulation synthesized by *Bolzan and Strobel* [1994] for Summit.

relation with the North Atlantic Oscillation (NAO) in this region [*Hurrell*, 1995; *Appenzeller et al.*, 1998].

4.3. Central Greenland

Estimates for central Greenland precipitation may be compared with the reliable time series compiled by *Bolzan and Strobel* [1994]. Their time series is a synthesis of nine ice cores surrounding Summit and provides a depiction of interannual variability that is valid for "grid box" length scales. Aside from the Keen model, which was tuned to the Bolzan and Strobel data, the average long-term value for Summit from atmospheric methods is 9 cm yr^{-1}. This ranges from the ERA 1979-1993 average of 12 cm yr^{-1} to the corrected NCEP data value of 7 cm yr^{-1} for 1958-1996. Again, the Bolzan and Strobel value is 22 cm yr^{-1}. As previously mentioned, this deficiency is at least partially due to errors in the topographies used. A similar comparison for the whole of the central region is shown in Table 2. There is agreement among nearly all of the data sets on an annual cycle for the central region, with larger values occurring during summer months. The exception is the derived atmospheric moisture budget *P–E*, which shows a semiannual oscillation with a minimum in July. This occurs both because of the effects of evaporation/sublimation as well as the lower resolution afforded by the moisture budget method, which erroneously introduces some of the annual cycle characteristics from southern Greenland.

Figure 13 shows a comparison of the temporal variability of methods which have significant overlap with the Bolzan and Strobel data for 1975-1986. The data have been nondimensionalized to remove the bias in the long-term values. In general, it is apparent that there is some convergence in each of the time series around 1981. This corresponds to the time when a significant reduction occurred in the number of missing observations for the Angmagssalik rawinsonde station (66°N, 38°W) [*Robasky and Bromwich*, 1994]. This, combined with the suggestion that topographic deficiencies in the southeast reduce plateau precipitation, implies that Summit precipitation contains a significant component originating from the southeast. Observational studies differ on whether Summit precipitation originates in the southeast [*Ohmura and Reeh*, 1991] or southwest [*Bolzan and Strobel*, 1994], however, and the present deficient data sets cannot be used to fully resolve this question. These difficulties have significant relevance to trajectory studies using the numerical analyses [e.g., *Kahl et al.*, 1997]. The concept that both moisture sources are significant is a view which may explain the difficulties in resolving Icelandic low variability from Summit glaciological data. A comprehensive review of these issues associated with Summit moisture sources is given by *Barlow et al.* [1997].

Recently, an update to the Summit record has been produced using additional glaciological data over a larger area [*Kuhns et al.*, 1997]. A comparison of this time series with the original Bolzan and Strobel data shows similar variability (r^2=0.67), although the amplitude is significantly smaller. The standard deviation of the normalized time series for the new accumulation data [*Kuhns et al.*, 1997, Figure 9] is about half of that for Bolzan and Strobel. It is apparent from Figure 13 that point values from the precipitation data sets show similar amplitude to that of Bolzan and Strobel and that a corresponding comparison with the Kuhns et al. data would require spatial averaging over an area similar to that used in their study. The larger area incurs the precipitation spatial gradient errors associated with the topography. This problem illustrates the importance of using accurate topographic data in the vicinity of Summit.

4.4. East-Central Greenland

The northeastern coast of Greenland is a significant region of transient forcing and cyclogenesis, as seen by the analysis of circulation conditions affecting the northern region.

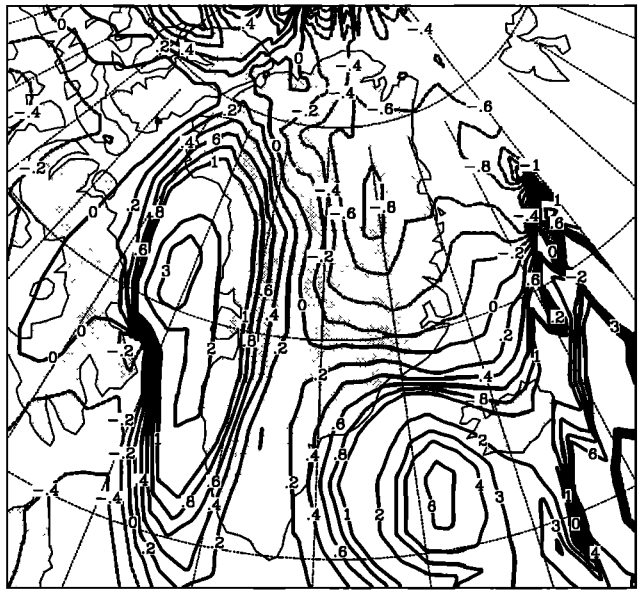

Figure 14. Average ratio of mean moisture convergence from ECMWF operational analyses divided by eddy convergence, averaged for 1985-1995. The contour interval is variable to show detail.

Calanca and Ohmura [1994] contrast eastern and western Greenland using the decomposition of the ECMWF analyses moisture budget. *Calanca and Ohmura* [1994] found that precipitation in the west-central region contained a larger component resulting from the mean circulation, while the eastern region experiences a net divergence of the mean moisture transport for the year. To evaluate the relative importance of the two components, the ratio of the average monthly mean divided by eddy moisture convergence from the ECMWF analyses is shown in Figure 14 for the 11-year period 1985-1995. For the west-central region over this time period the mean circulation component of the atmospheric moisture convergence becomes as large as 3 times the transient component over the Baffin Bay, a surprising value, given the number of cyclones found to propagate through the region. *Calanca and Ohmura* [1994] indicate that western Greenland precipitation is primarily the result of the orographic influence of the Greenland Ice Sheet. In contrast, the precipitation of the east-central region is seen as the difference of large positive eddy convergence and large negative mean convergence. This results in the very small values over the central plateau and the northeast coast. This balance changes slightly in nature after 1990, however. Figure 15 shows a time series of the moisture budget $P-E$ for the east-central region in comparison to the forecast P of the ERA. It is seen that the nature of the $P-E$ curve changes from containing substantial negative values prior to 1991 to entirely positive values afterward. The last negative value occurs in November 1990. The average prior to 1991 is 9 cm yr^{-1} compared to 27 cm yr^{-1} thereafter. The ERA do not show any similar trend in forecast P. The ERA forecast E was also evaluated for this region and was found to be slightly increasing over the same period at an insignificant rate, in disagreement with the operational analyses time series. The other precipitation methods also fail to show this change. As the total convergence for this region results from the relatively small difference between two large components, it is suggested that this has the effect of amplifying changes to the data assimilation system, which are manifested in the mean transport component. Several changes to the ECMWF data assimilation system occurred during 1991, including a doubling of the spatial resolution [*Trenberth*, 1992]; it is not immediately clear which specific adjustment is the cause.

Because of this unusual balance, *Calanca and Ohmura* [1994] find a highly variable annual cycle for the region. Surprisingly, most of the methods agree on minima in May and October when averaged over for the period 1985-1993; there is no obvious month for maximum precipitation.

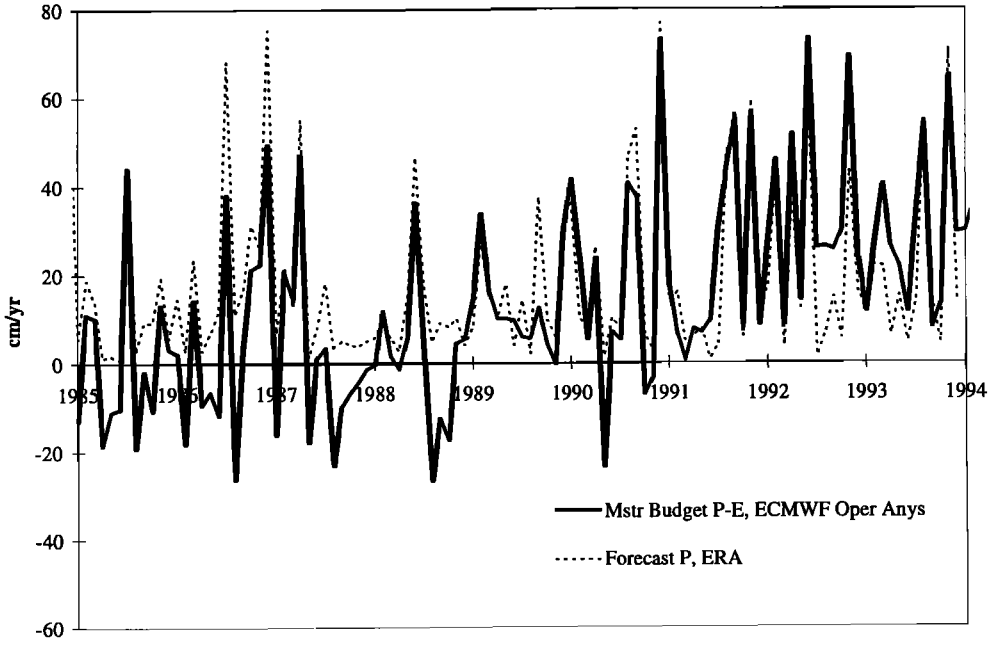

Figure 15. Comparison of $P-E$ computed from ECMWF operational analyses and ERA forecast P for the region defined as east-central in Figure 1, in cm yr^{-1}.

Qualitatively, this is in agreement with averaged gauge data from Danmarkshavn (77°N, 19°W) [*Berthelsen et al.*, 1993]. The east-central region as well as the southern region, discussed below, demonstrate the first-order weakness of the Keen model. The formulation of the Keen model shown in equation (3) is strongly dependent on the annual cycle of the low-level specific humidity field, which typically produces an annual cycle with a July maximum. Here the Keen model shows a definite maximum precipitation rate of about 55 cm yr^{-1} occurring in July, while Keen values for September through May average about half this rate. Thus the Keen model has significant difficulty with regions where the precipitation and specific humidity annual cycles differ markedly. There is a similar distribution of long-term values for the east-central region among the various methods, ranging from 13 cm yr^{-1} for the corrected NCEP data to 29 cm yr^{-1} for the Keen model. As shown in Table 2, the long-term glaciological value is near the center of these estimates at 18 cm yr^{-1}.

4.5. Southern Greenland

Southern Greenland is influenced by mean circulation associated with the Icelandic low, as well as the cyclonic activity associated with the North Atlantic storm track. The influence of the storm track is reviewed by *Chen et al.* [1997]. A principal precipitation mechanism is lee cyclogenesis occurring along the southeastern coast. Because of its close proximity to the storm track core and the relatively warm sea surface temperatures of the adjacent North Atlantic, there is a small component of convective precipitation in southern Greenland which is not found for the rest of the island. This is shown in Figure 16 from the ERA forecast fields. The convective amount applies to the southeastern most region and amounts to about 10 cm yr^{-1}. This is small in comparison to the total amount and slightly diminishes the value of methods which do not explicitly address the convective precipitation, such as the Chen-Bromwich method.

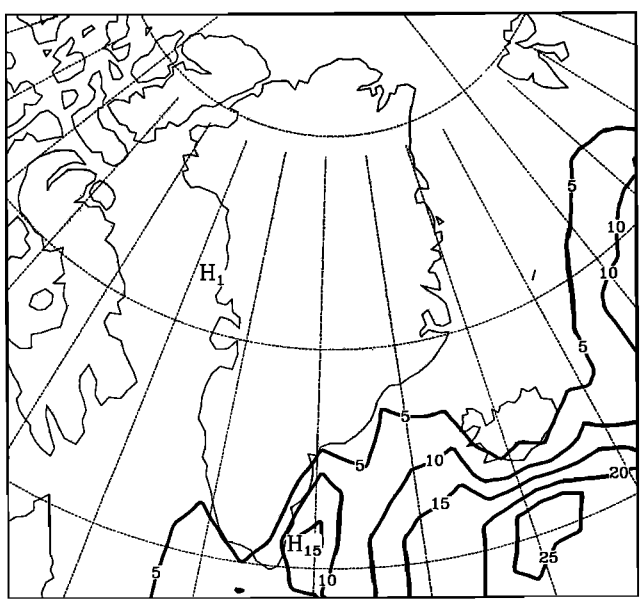

Figure 16. Average annual convective precipitation from ERA forecasts for 1979-1993. The contour interval is 5 cm yr^{-1}.

Additionally, the average annual cycle for southern Greenland is opposite in phase to that of the 700 hPa specific humidity, creating significant problems for the Keen model. Finally, E is also significant for the southern region, as previously found in Figure 4.

The annual precipitation cycle is characterized by a minimum in July with maximum values in the winter months [*Berthelsen et al.*, 1993]. With the exception of the Keen model, there is reasonable agreement among the various methods for the annual cycle averaged for 1985-1993. The average seasonality index among methods in agreement is 0.7, with the Keen model showing larger summer values and a 1.7 seasonality index. The ECMWF moisture budget $P-E$ has an index value which is slightly closer to unity, with a 0.8 value. This is somewhat surprising given the larger values of E occurring in summer. For the years 1985-1993 the various methods produce a range of mean annual values which is approximately 25% of the average for all methods (64 cm yr^{-1}). The glaciological value is low for the south due to the significant liquid precipitation component and measurement difficulties for this region (Table 2). There are substantial differences in the interannual variability. In particular, the Chen-Bromwich data show substantial downward trend of about 1.7 cm yr^{-1} for the region, while other methods show a small upward trend over the same time period. The downward trend in the Chen-Bromwich data is biased by very large values for 1985-86. The Chen-Bromwich model incorporates ECMWF operational analyses, however there is no similar trend in the $P-E$ moisture budget derived from the ECMWF operational analyses. This contrast with the Chen-Bromwich data for this region requires further consideration.

5. Status of Greenland Precipitation Retrieval

The previous sections describe the regional discrepancies associated with the precipitation data. The individual characteristics of each of the regions and their close proximity illustrate the tremendous challenge in obtaining an accurate spatial and temporal depiction of Greenland precipitation. In general, the following comments are given regarding each of the analysis data sets.

The derived moisture budget from ECMWF operational analyses is a valuable data set. The total moisture flux, and the Reynolds decomposition of the moisture transports, yields important information regarding the physical mechanisms responsible for precipitation on the Greenland Ice Sheet. As with other methods, the analyses' use of an inaccurate topographic data set results in some deficiencies in comparison to glaciological data. In particular, the interior plateau is too dry. For these data, the plateau shortfall may also be due to inadequate vertical resolution. Changes to the data assimilation scheme create some ambiguity for assessing trends and interannual variability, however. The east-central region in particular is susceptible to these changes because of its unique balance of mean versus eddy transport. The derivation of the moisture transports shown here and by *Calanca and Ohmura* [1994] is computationally practical but produces a very low resolution depiction, which tends to blur the localized precipitation characteristics. Higher spatial resolution is possible, for example, if the spectral format of the ECMWF data is used at full resolution, but it is unclear if this would necessarily resolve the important features.

Forecast fields derived from reanalysis data eliminate spurious trends associated with changes to the operational analysis data sets. For the NCEP/NCAR data, there are significant spatial problems associated with the numerical weather prediction model used. The corrected NCEP P is an improvement but creates fields that are overly dry north of 70°N. Despite the spatial representation problems, there is excellent agreement with ERA for the whole of Greenland for seasonal and interannual variability. On regional scales, the corrected NCEP data differ for the northern region on the seasonality of the annual cycle. Additionally, the ERA data are too dry for the interior plateau. As an aside, it should be noted that ECMWF has recently addressed deficiencies in the model topography used in both daily operations and the upcoming ERA-40 project (R. Gibson, personal communication, 1998).

From this study it is found that the enhanced precipitation methods appear to be the most useful for obtaining high-resolution spatial depictions of the ice sheet surface. At present, the use of operational analyses and a deficient topographic data set for the Chen-Bromwich model partially compromise the resulting data set. Nevertheless this method is found to be less susceptible to data artifacts than the atmospheric moisture budget and the Keen model. Revision of this data set incorporating the errors identified will provide a realistic, high-resolution climatological record of Greenland precipitation. Apart from the frequently used long-term spatial depictions obtained from glaciological data, this study demonstrates that a suite of additional minimum criteria are available for the validation of precipitation fields. This includes the regional annual cycles, which may be qualitatively inferred from the long-term coastal gauge averages, as shown by the *Berthelsen et al.* [1993] Greenland Atlas. Additionally, there are the time series at Summit and the relative roles of mean and transient contributions. It remains to be seen whether corrections to model topographies will improve central Greenland values for all methods. If not, then alternative explanations including the role of upslope snowdrift, as suggested by *Bergeron* [1965], must be considered.

We finally review previous long-term results extending prior to 1979, as discussed by *Bromwich et al.* [1993]. Using the Keen model, it was found that Greenland precipitation showed a downward trend from 1964 to 1976, with a slight upward trend thereafter. The overall precipitation trend presented by the Keen model is consistent with the declining annual surface temperature observed for southern Greenland over a similar time period [*Chapman and Walsh*, 1993]. At present, the only other data set available to cover this period is the NCEP/NCAR reanalysis. Figure 17 shows a comparison of annual values for these data as well as other methods for more recent years. For the period 1977 to 1988 there is a small upward increase in both the Keen model and the NCEP/NCAR P of 0.6 and 0.2 cm yr^{-1}, respectively. It can be seen, however, that there are some differences in the two curves prior to 1981. These differences are primarily due to variability in the low precipitation months of early spring. Figures 17b and 17c show the time series of minimum and maximum precipitation months, respectively. There are clear differences for the March time series in 1975 and 1976. It should be noted that the 1976 and 1977 NCEP/NCAR data were recently reprocessed to correct for assimilation errors. This time series uses the reprocessed fields. For August there is reasonable agreement beginning in 1973 between the two

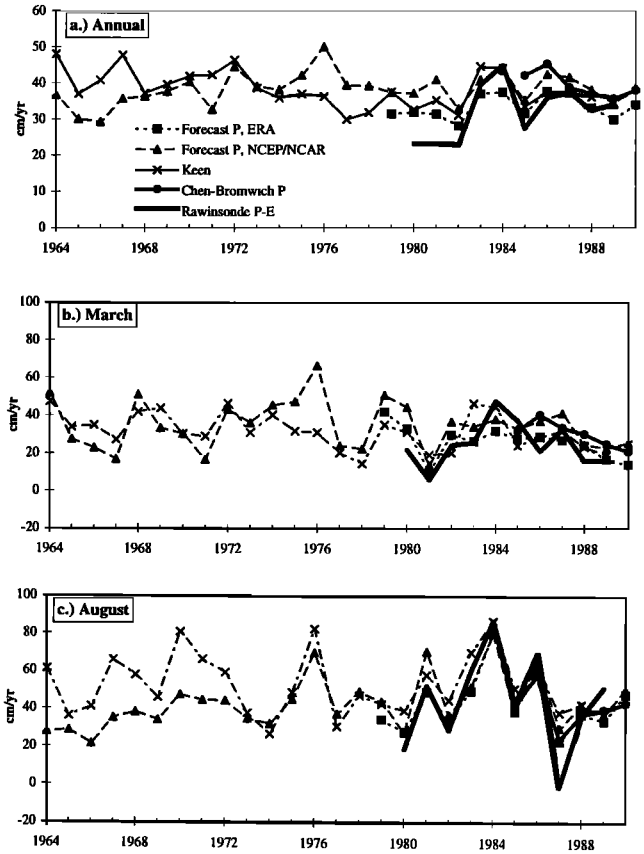

Figure 17. Time series of (a) annual, (b) March, and (c) July precipitation estimates for Greenland, in cm yr^{-1}.

methods. The agreement indicates that a cancellation of regional errors occurs when the entire island is considered. The onset of the agreement between the two time series in 1973 corresponds to the time of the inclusion of significant level height data in the NCAR archive [*Robasky and Bromwich*, 1994]. The additional data provided by rawinsonde significant levels are important for the accurate initialization of the numerical weather prediction model and for moisture budget computations; the Keen model is independent of these data, however. From this comparison it is concluded that the *Bromwich et al.* [1993] time series appears to be reasonable from 1973 onward and that significant difficulties would be incurred by other methods in establishing the time series prior to this date.

Notation

ECMWF European Centre for Medium-Range Weather Forecasts.
ERA ECMWF reanalysis project.
GIMEX Greenland Ice Margin Experiment.
GPCC Global Precipitation Climatology Centre.
NAO North Atlantic Oscillation.
NCAR National Center for Atmospheric Research.
NCEP National Centers for Environmental Prediction (formerly NMC).
NMC National Meteorological Center (now NCEP).
PARCA Program for Arctic Regional Climate Assessment.
VFI vorticity flux index.

Acknowledgments. The authors thank Hong Xu of the Department of Geography, The Ohio State University, for assistance with analysis and figures of the Csathó-PARCA data set. ECMWF analyses were obtained from NCAR. This research was sponsored by the National Aeronautics and Space Administration under grant NAGW 3677 to the first author. This is contribution 1094 of the Byrd Polar Research Center.

References

Alley, R.B., et al., Abrupt increase in Greenland snow accumulation at the end of the Younger Dryas event, *Nature*, *362*, 527-529, 1993.

Appenzeller, C., J. Schwander, S. Sommer, and T.F. Stocker, The North Atlantic Oscillation and its imprint on precipitation and ice accumulation in Greenland, *Geophys. Res. Lett.*, *25*, 1939-1942, 1998.

Barlow, L.K., J.C. Rogers, M.C. Serreze, and R.G. Barry, Aspects of climate variability in the North Atlantic sector: Discussion and relation to the Greenland Ice Sheet Project 2 high-resolution isotopic signal, *J. Geophys. Res.*, *102*, 26,333-26,344, 1997.

Bender, G., The distribution of snow accumulation on the Greenland Ice Sheet, 110 pp., M.S. thesis, Geophys. Inst., Univ. of Alaska, Fairbanks, 1984.

Bergeron, T., The possible role of snowdrift in building up high inland ice-sheets, *Prog. Oceanogr.*, *3*, 385-390, 1965.

Berthelsen, C., I. Holbech Mortensen, and E. Mortensen, *Kalaallit Nunaat (Greenland Atlas)*, 127 pp., Greenl. Home Rule Gov., Nuuk, 1993.

Bolzan, J.F., and M. Strobel, Accumulation rate variations around Summit, Greenland, *J. Glaciol.*, *40*, 56-66, 1994.

Bradley, R.S., and J.K. Eischeid, Aspects of the precipitation climatology of the Canadian High Arctic, in *Glacial Geologic and Glacio-Climatic Studies in the Canadian High Arctic*, edited by R.S. Bradley, pp. 250-271, Dep. Geol. and Geogr., Univ. of Mass., Amherst, 1985.

Broecker, W.S., Thermohaline circulation, the achilles heel of our climate system, Will man-made CO_2 upset the current balance, *Science*, *278*, 1582-1588, 1997.

Bromwich, D.H., F.M. Robasky, R.A. Keen, and J.F. Bolzan, Modeled variations of precipitation over the Greenland Ice Sheet, *J. Clim*, *6*, 1253-1268, 1993.

Calanca P., and A. Ohmura, Atmospheric moisture flux convergence and accumulation on the Greenland Ice Sheet, in *Snow and Ice Covers, Interactions With the Atmosphere and Ecosystems*, edited by H.G. Jones, T.D. Davies, A. Ohmura, and E.M. Morris, pp. 77-84, *IAHS Publ. 223*, Int. Assoc. of Hydrol. Sci., Wallingford, England, 1994.

Chapman, W.L., and J.E. Walsh, Recent variations of sea ice and air temperature in high latitudes, *Bull. Am. Meteorol. Soc.*, *74*, 33-47, 1993.

Chen, Q.-s., D.H. Bromwich, and L. Bai, Precipitation over Greenland retrieved by a dynamic method and its relation to cyclonic activity. *J. Clim.*, *10*, 839-870, 1997.

Csathó, B., H. Xu, R. Thomas, D. Bromwich, and Q.-S. Chen, Comparison of accumulation and precipitation maps of the Greenland Ice Sheet, *Eos. Trans. AGU*, *78*(46), Fall. Meet. Suppl., F9, 1997.

Dodd, J.P., and I.N. James, Diagnosing the global hydrological cycle from routine atmospheric analyses, *Q. J. R. Meteorol. Soc.*, *122*, 1475-1499, 1996.

Duchon, C.E., Lanczos filtering in one and two dimensions, *J. Appl. Meteorol.*, *18*, 1016-1022, 1979.

Duynkerke, P.G., and M.R. van den Broeke, Surface energy balance and katabatic flow over glacier and tundra during GIMEX-91, *Global Planet. Change*, *9*, 17-28, 1994.

Ekholm, S., A full coverage, high-resolution, topographic model of Greenland computed from a variety of digital elevation data, *J. Geophys. Res.*, *101*, 21,961-21,972, 1996.

Elliott, W.P., and D.J. Gaffen, On the utility of radiosonde humidity archives for climate studies. *Bull. Am. Meteorol. Soc.*, *72*, 1507-1520, 1991.

Fisher, D.A., R.M. Koerner, K. Kuivinen, H.B. Clausen, S.J. Johnsen, J.-P. Steffensen, N. Gundestrup, and C.U. Hammer, Inter-comparison of ice core $\delta(^{18}O)$ and precipitatation records from sites in Canada and Greenland over the last 3500 years and over the last few centuries in detail using EOF techniques, in *Climatic Variations and Forcing Mechanisms of the Last 2000 Years*, *NATO Adv. Sci. Inst. Ser.*, vol. I 41, edited by P.D. Jones, R.S. Bradley, and J. Jouzel, pp. 297-328, Springer-Verlag, New York, 1996.

Genthon, C., and A. Braun, ECMWF analyses and predictions of the surface climate of Greenland and Antarctica, *J. Clim.*, *8*, 2324-2332, 1995.

Gibson, J.K., A. Hernandez, P. Kållberg, A. Nomura, E. Serrano, and S. Uppala, Current status of the ECMWF Re-Analysis Project, in *Seventh Sympium on Global Change Studies*, pp. 112-115, Am. Meteorol. Soc., Boston, Mass., 1996.

Hurrell, J.W., Decadal trends in the North Atlantic Oscillation, Regional temperatures and precipitation, *Science*, *269*, 676-679, 1995.

Kahl, J.D.W., D.A. Martinez, H. Kuhns, C.I. Davidson, J.-L. Jaffrezo, and J.M. Harris, 1997: Air mass trajectories to Summit, Greenland: A 44-year climatology and some episodic events. *J. Geophys. Res.*, *102*, 26,861-26,875, 1997.

Kalnay, E., et al., The NCEP/NCAR 40-year reanalysis project, *Bull. Am. Meteorol. Soc.*, *77*, 437-471, 1996.

Keegan, T.J., Arctic synoptic activity in winter, *J. Meteorol.*, *15*, 513-521, 1958.

Keen, R.A., Statistical-dynamical model of accumulation on the Greenland Ice Sheet, *Ann. Glaciol.*, *5*, 69-74, 1984.

Kuhns, H., C. Davidson, J. Dibbs, C. Stearns, M. Bergin, and J.-L. Jaffrezo, Temporal and spatial variability of snow accumulation in central Greenland, *J. Geophys. Res.*, *102*, 30,059-30,068, 1997.

Loewe, F., The transport of snow on ice sheets by wind, in *Studies on Drifting Snow*, Publ. 13, edited by U. Radok, section II, 69 pp., Meteorol. Dep., Univ. Melbourne, 1970.

Meesters, A., Dependence of the energy balance of the Greenland ice sheet on climate change: Influence of katabatic wind and tundra, *Q. J. R. Meteorol. Soc.*, *120*, 491-517, 1994.

Mo, K.C., and R.W. Higgins, Large-scale atmospheric moisture transport as evaluated in the NCEP/NCAR and the NASA/DAO reanalyses, *J. Clim.*, *9*, 1531-1545, 1996.

National Snow and Ice Data Center, Digital SAR Mosaic and Elevation Map of the Greenland Ice Sheet, CD-ROM, NSIDC Distrib. Activ. Arch. Cent., Univ. of Colo., Boulder, 1997.

Ohmura, A., and N. Reeh, New precipitation and accumulation maps for Greenland, *J. Glaciol.*, *37*, 140-148, 1991.

Ohmura, A., M. Wild, and A. Bengtsson, A possible change in mass balance of Greenland and Antarctic Ice Sheets in the coming century, *J. Clim.*, *9*, 2124-2135, 1996.

Oki T., K. Musiake, K. Masuda, and H. Matsuyama, Global runoff estimation by atmospheric water balance using ECMWF data set, in *Macroscale Modelling of the Hydrosphere*, edited by W.B. Wilkinson, pp. 163-171, *IAHS Publ. 214*, Inst. Assoc. of Hydrol. Sci., Wallingford, England, 1993.

Radok, U., R.G. Barry, D. Jenssen, R.A. Keen, G.N. Kiladis, and B. McInnes, *Climatic and Physical Characteristics of the Greenland Ice Sheet*, 193 pp., CIRES, Univ. of Colo., Boulder, 1982.

Reeh, N., Calving from Greenland glaciers: Observations, balance estimates of calving rates, calving laws, in *Report on the Workshop on the Calving Rate of West Greenland Glaciers in Response to Climate Change*, edited by N. Reeh, pp. 85-102, Dan. Polar Cent., Copenhagen, 1994.

Robasky, F.M., and D.H. Bromwich, Greenland precipitation estimates from the atmospheric moisture budget. *Geophys. Res. Lett.*, *21*, 2495-2498, 1994.

Rudolf, B., H. Hauschild, W. Rueth, and U. Schneider, Terrestrial precipitation analyses: Operational method and required density of point measurements, in *Global Precipitations and Climate Change*. *NATO Adv. Sci. Inst. Ser.*, vol. I 26, edited by M. Desbois, and F. Desalmand, pp. 173-186, Springer-Verlag, New York, 1994.

Schwerdtfeger, W., *Weather and Climate of the Antarctic*, *Dev. Atmos. Sci.*, vol. 15, 261 pp., Elsevier, New York, 1984.

Serreze, M.C., and R.G. Barry, Synoptic activity in the Arctic basin, 1979-85, *J. Clim.*, *1*, 1276-1295, 1988.

Serreze, M., and J. Maslanik, Arctic precipitation as represented in the NCEP/NCAR reanalysis, *Ann. Glaciol.*, *25*, 429-433, 1997.

Serreze, M.C., R.G. Barry, and A.S. McLaren, Seasonal variations in sea ice motion and effects on sea ice concentration in the Canada basin, *J. Geophys. Res.*, *94*, 10,955-10,970, 1989.

Shuman, C.A., R.B. Alley, S. Anandakrishnan, J.W.C. White, P.M. Grootes, and C.R. Stearns, Temperature and accumulation at the Greenland Summit: Comparison of high-resolution isotope profiles and passive microwave brightness temperature trends, *J.Geophys. Res.*, *100*, 9165-9177, 1995.

Stendel, M., and K. Arpe, Evaluation of the hydrologic cycle in reanalyses and observations, *Tech. Rep.*, 52 pp., Max-Planck-Inst. für Meteorol., Hamburg, 1997.

Thompson, S.L., and D. Pollard, Greenland and Antarctic mass balances for present and doubled atmospheric CO_2 from GENESIS Version-2 global climate model, *J. Clim.*, *10*, 871-900, 1997.

Trenberth, K.E., Global analyses from ECMWF and atlas of 1000 to 10 mb circulation statistics, *NCAR Tech. Note, NCAR/TN-373+STR*, 191 pp. plus 24 fiche, Natl. Cent. for Atmos. Res., Boulder, Colo., 1992.

Trenberth, K.E., Using atmospheric budgets as a constraint on surface fluxes, *J. Clim.*, *11*, 2796-2809, 1997.

Trenberth, K.E., and C.J. Guillemot, Evaluation of the global atmospheric moisture budget as seen from analyses, *J. Clim.*, *8*, 2255-2272, 1995.

Trenberth, K.E., and C.J. Guillemot, Evaluation of the atmospheric moisture and hydrologic cycle in the NCEP reanalyses, *NCAR Tech. Note, NCAR/TN-430+STR*, 308 pp., Natl. Cent. for Atmos. Res., Boulder, Colo., 1996.

van den Broeke, M.R., P.G. Duynkerke, and J. Oerlemans, The observed katabatic flow at the edge of the Greenland ice sheet during GIMEX-91, *Global Planet. Change*, *9*, 3-15, 1994.

Warrick, R.A., C. Le Provost, M.F. Meier, J. Oerlemans, and P.L. Woodworth, Changes in sea level, in *Climate Change 1995, The Science of Climate Change: Contribution of Working Group 1 to the Second Assessment Report of the Intergovernmental Panel on Climate Change*, edited by J.T. Houghton, L.G. Meira Filho, B.A. Callandar, N. Harris, A. Kattenberg, and K. Maskell, pp. 359-405, Cambridge Univ. Press, New York, 1995.

Woo, M.-K., R. Heron, P. Marsh, and P. Steer, Comparison of weather station snowfall with winter snow accumulation in high Arctic basins, *Atmos. Ocean*, *32*, 733-755, 1983.

Zwally, H.J., and M.B. Giovinetto, Accumulation in Antarctica and Greenland derived from passive-microwave data: A comparison with contoured compilations, *Ann. Glaciol.*, *21*, 123-130, 1995.

D.H. Bromwich, R.I. Cullather, and Q.-s. Chen, Polar Meteorology Group, Byrd Polar Research Center, The Ohio State University, 1090 Carmack Rd., Columbus, OH 43210-1002. (e:mail: bromwich@polarmet1.mps.ohio-state.edu)

B.M. Csathó, Remote Sensing Laboratory, Byrd Polar Research Center, The Ohio State University, 1090 Carmack Rd., Columbus, OH 43210-1002.

(Received March 17, 1998; revised June 29, 1998;
accepted July 7, 1998.)